

Vision enhancement through single image fog removal

T.LEELAVATHI ,19HU1D3802,DECS, Department of ECE, TECH, Tadipatri.

R.SREENIVASULU,Associate Professor, Department of ECE, TECH, Tadipatri.



a b s t r a c t

Contrast and color of the captured pictures are degraded under foggy weather conditions and this degradation is often attributed to attenuation and airlight. To reduce the number of road accidents through vision enhancement in turbid weather, an efficient fog removal technique plays a vital role as fog greatly reduces the visibility and hence affects the computer vision algorithms such as surveillance, tracking and Fog Vision Enhancement System (FVES). In this paper, a novel and effective algorithm is proposed for single image fog removal that's capable of handling images of gray and color channels. The proposed algorithm introduces Dark Channel Prior (DCP) followed by Weighted Least Square (WLS) and High Dynamic Range (HDR) based fog removal scheme. The qualitative and quantitative analysis is applied for the assessment of defogged images obtained from the proposed methodology and is additionally compared with the different fog removal algorithms to establish its superiority. The foremost dominant advantage of the proposed algorithm is its capability to preserve sharp details whereas maintaining the color quality.

Keywords:

Air-light
Contrast gain
Colorfulness index
High Dynamic Range
Weighted Least Square
Transmission map
Dark Channel Prior

1. Introduction

The image qualities of captured outdoor scenes are usually degraded due to bad weather such as fog, haze, smog, cloud and rain. Bad weather reduces visibility and contrast of the scene. Visibility range is greatly affected by fog as compared to other turbid weather conditions. For road traffic, fog can be categorized as low fog (visibility range, 300–1000 m) and dense fog (visibility range < 100m). Visibility degradation due to bad weather is one of the biggest causes of road fatal injuries across the world. National Highway Traffic Safety Administration (NHTSA) statistics showed that 25% and 28% fatal crashes out of total accidents occurred in the USA during 2012 and 2013, respectively. World Health Organization (WHO) also declared, one person is killed every 25 s due to road injuries.

The atmospheric particles, mainly water droplets causes, absorption and scattering. Where there is scattering, two fundamental phenomena attenuation and airlight exist and the resulting light coming towards the camera or the observer from the scene gets attenuated due to scattering through water droplets and thus degrades the image quality of an outdoor scene. Diminishing the contrast due to scattering is termed as attenuation. The whiteness

effect in the scene towards the observer or the camera is known as airlight. These two phenomena jointly produce a degraded image. It is observed that attenuation and airlight are the functions of the distance between camera and scene. Hence depth map estimation is required for restoring true scene. With the advancement in every field of image processing and computer vision from last few decades, it is possible to visualize even in bad weather with little degradation but the performance of many computer vision applications, such as object detection and tracking, video surveillance, FVES and target identification may fail due to degraded images, therefore improving visibility through fog removal is an inevitable task. These applications are meant to recognize vehicles, traffic signs, and signals clearly through vision enhancement using fog removal.

With the advancement of technology, many single image fog removal methods [2,3,4,5,8,17] have been proposed. Fattal [2] proposed a method based on Independent Component Analysis (ICA) to estimate transmission map where restoration was based on color information and hence can't be applied to the gray image and dense fog because dense fog is colorless. Tarel and Hautiere [3] proposed a fast visibility restoration method based on linear operations but requires many parameters for adjustment. This fast algorithm paved the way for real-time implementation. He et al. [4] proposed a very simple but effective single-image haze removal method using DCP and refined by soft matting. DCP is a kind of statistics of outdoor haze-free images that contain some pixels whose intensity is very low in at least one channel. Using this prior

technique, direct estimation of airlight map is possible and a high quality haze-free image is recovered but fails when the brightness of scene object is very close to the atmospheric light. Tripathi and Mukhopadhyay [5] proposed a novel, efficient fog removal algorithm that uses anisotropic diffusion with the additional use of histogram equalization and stretching as pre-processing and post-processing steps respectively. The parameters and constants remain the same irrespective of the density of fog. A multi-scale fusion based approach is presented for dehazing [6,7]. It was derived by white balancing and a contrast enhancing using two original degraded images. Fattal [8] again proposed a new dehazing method for a color image using a local color-line model that exhibit a 1D distribution of pixels of small image patches. These color-lines are used to estimate the transmission map of a scene. He used a variable gamma correction factor to restore the color images with high accuracy at low noise levels only, but sky region in the image limits the performance of color-line dehazing algorithm like other methods. M. Negru et al. [17] proposed an exponential contrast restoration method in daytime fog for driver assistance, taking into account the variation in fog density as a function of distance.

In this paper, a novel fog removal technique is proposed which produces a more enhanced edge-preserving image without using any pre-processing technique like histogram equalization [5]. Proposed algorithm uses DCP principle at initial stage followed by High Dynamic Range (HDR) tone mapping using Weighted Least Squares (WLS) for contrast adjustment and to visualize the fine detail within an image respectively. HDR images represent original light values captured for the scene while WLS is an edge preserving filter which computes detail layers and recombines them with strong fine detail. A WLS filter that is close to anisotropic diffusion was used previously to diminish ringing effect [9] while de-blurring images in the presence of noise. The proposed algorithm can be applied to color images as well as single color channel grayscale foggy images and consists of fewer known variables than unknown ones, which is an ill-posed problem. However, basic physics for observation can be considered as clues while user intervention is not required for the proposed algorithm.

This paper is organized into five sections. In the next section (section II) of this paper, we explain in detail the proposed fog removal algorithm which consists of airlight map estimation, transmission map estimation, and refinement procedure. In section III, contrast manipulation with preserving fine details using HDR and WLS scheme contributes as post-processing step is discussed. Further in section IV, simulation and results with quantitative analysis using performance metrics are discussed and compared with the state of the art. The remainder of this paper concludes and shows future scope.

2. Defog algorithm

The flow of the proposed fog removal method in the form of the block diagram is shown in Fig. 1. It contains the initial estimation of atmospheric light and air-light, transmission estimation with a refined map and restoration followed by post-processing. The concept of defogging algorithms for images originate from an atmospheric scattering model was proposed by Koschmieder [10]. According to Koschmieder's law [1,3], the effect of fog or haze is represented as:

$$I_{\delta; j\mathcal{P}} \approx I_{\text{attenuate}}(\delta; j\mathcal{P}) + A_{\text{air-light}}(\delta; j\mathcal{P}) \tag{1}$$

In the above equation, two right-hand side terms, attenuation and air-light are the functions of distance from camera to the scene represented as:

$$I_{\text{attenuate}}(\delta; j\mathcal{P}) \approx I_0(\delta; j\mathcal{P}) e^{-b d(\delta; j\mathcal{P})} \tag{2}$$

$$A_{\text{air-light}}(\delta; j\mathcal{P}) \approx I_1 \left(1 - e^{-b d(\delta; j\mathcal{P})} \right) \tag{3}$$

where, $I_{\text{attenuate}}(\delta; j\mathcal{P})$ is the attenuated image intensity at pixel $\delta; j\mathcal{P}$ in poor weather, mostly hazy and foggy in nature and $I_0(\delta; j\mathcal{P})$ is the image intensity of the de-weathered image. b is the extinction or atmospheric scattering coefficient based on the wavelength of light function, which is related to the fog concentration and reflects the optical absorption of aerosol in the air and determines the atmospheric visibility. $d(\delta; j\mathcal{P})$ is the distance of the scene point from a camera and I_1 is the global atmospheric constant or sky intensity.

More simply fog model can be represented [4,16] as:

$$I_{\delta; j\mathcal{P}} \approx I_0 \delta z \rho + A \delta_1 - t \delta z \rho \tag{4}$$

where, $I_{\delta; j\mathcal{P}}$ is observed a foggy image, $I_0 \delta z \rho$ is scene radiance or reflectance (fog-free image as desired), A is the global atmospheric light or skylight and $t \delta z \rho$ represents the transmission parameter, the portion of light which directly goes towards observer without scattering in the medium.

The fog-free image is restored as follows:

$$I_0 \delta z \rho \approx \frac{I_{\delta; j\mathcal{P}} - A}{t \delta z \rho} \tag{5}$$

This model is also applicable to a color image by applying this on each RGB component. After getting a poor contrast-restored image, contrast enhancement with fine detail is required and that is possible by converting the defogged image into HDR and applying WLS filter. A combined post-processing technique which includes HDR with WLS is used for the first time in this paper for fog removal to obtain clear sharp images while preserving color quality.

2.1. Initial estimation of atmospheric and Air-light

After normalizing the image, the pixels with highest intensity out of 0.1% brightest pixels that are close to 1 are treated as sky-light assuming that the color of atmospheric light is very close to the color of the sky and is always a positive quantity. As the dark channel is mentioned as the minimum intensity across RGB channels as at least one color channel have very low values close to zero.

$$\text{Dark channel } \approx \min_{c \in \{r, g, b\}} \min_{\delta; j\mathcal{P}} I_c(\delta; j\mathcal{P}) > 0 \tag{6}$$

where I_c is a color channel of an RGB image, $c \in \{r, g, b\}$ is used to find the minimum value in the color channels, the second 'min' operator behaves as a minimum filter across a local patch $\Omega(z)$, centered at z . The key observation of Dark Channel Prior is based on haze-free outdoor scenes. The dark channel of a haze-free image has a very low intensity values close to zero and looks very dark. This can be used for defogging. Dark channel can be also used to estimate more reliable value of air-light and found as the minimum of the brightest pixels of the input foggy image [4]. This minimized pixel extraction is a more robust technique for airlight estimation than simple brightest pixel method.

2.2. Transmission estimation

Transmission estimation is important to measure the fog thickness. Transmission map, $t(z)$ is the fraction of light that reaches observer without scattering. For the estimation of $t(z)$, the value of atmospheric light in Dark Channel Prior of (6) is used with a constant local patch but it is not necessarily always constant. The size of the local patch depends upon the specific application.

Therefore, min operator is used in the local window on the input degraded image by dividing the previously obtained

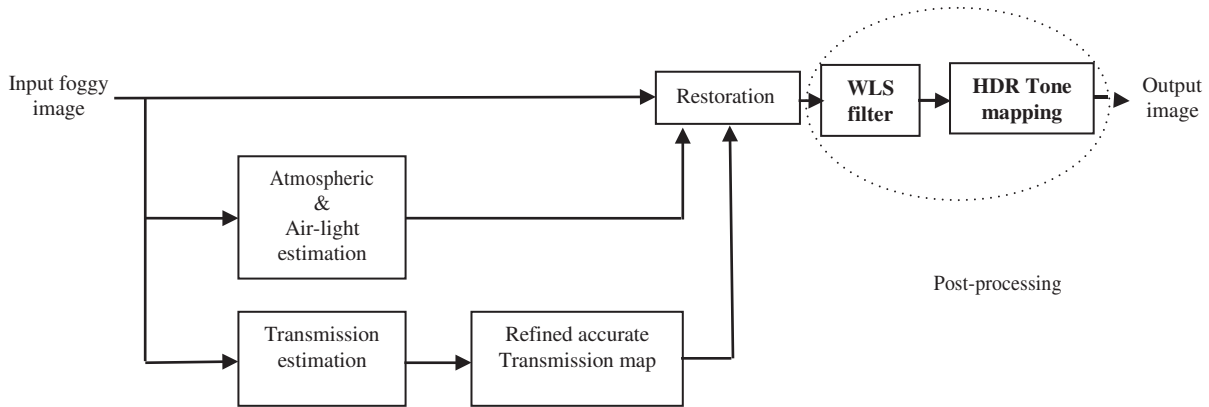


Fig. 1. Block diagram of the proposed fog removal algorithm.

atmospheric light in all the three color channels respectively. So, the fog model (4) becomes:

$$\min_{c \in \{R, G, B\}} \frac{\sum_z I_0(z) \cdot t(z)}{A} \quad \min_{c \in \{R, G, B\}} \frac{\sum_z I_0(z) \cdot t(z)}{A} \quad (7)$$

As the atmospheric light, A is a positive quantity and as the dark channel of fog-free image, $I_0(z)$ nearly equal to zero, then

$$\min_{c \in \{R, G, B\}} \frac{\sum_z I_0(z) \cdot t(z)}{A} \quad \text{yields } t(z) = 0 \quad (8)$$

Now using (7) and (8), the transmission $t(z)$ can be obtained as:

$$t(z) = 1 - \min_{c \in \{R, G, B\}} \frac{\sum_z I_0(z)}{A}; \quad \text{where: } 0 < t(z) < 1 \quad (9)$$

- $t(z) = 0$; fully foggy or opaque image
- $t(z) = 1$; completely fog free image

To get the transmission map for images without sky region is possible using (9) but it is not always suitable for images with sky region like road images as a front view from a vehicle. It depends on the portion of sky region included. To perceive the scene depth, it is mandatory to preserve a little quantity of fog that can vary according to the entropy of the foggy image. If the entropy is smaller, that quantity is closer to 1 and for higher entropy foggy images it is set nearer to 0. Therefore, Eq. (9) will be modified as:

$$t(z) = 1 - x \cdot \min_{c \in \{R, G, B\}} \frac{\sum_z I_0(z)}{A}; \quad 0 < x < 1 \quad (10)$$

where x is the fog intensity based information factor within that image. Here in this article, we set this value at 0.9 to get accurate transmission map with the sky region and it becomes brighter and smoother but most of the previous literature has fixed it at 0.95 [4]. Using $x = 0.95$ in Eq. (10) keeps a slight amount of fog effect around at all depths. The value of x sometimes needs to be decreased for substantial sky regions in an image, otherwise the sky region may create more artifacts. Simulation results with varying x are shown in Fig. 2. The obtained transmission map contains some artifacts due to the variability of transmission in every patch. So, refinement is a necessary task to overcome block artifacts. Laplacian estimation [11] is used for refinement next to transmission estimation to get more accurate transmission map.

2.3. Getting accurate transmission map

To minimize the artifacts produced in the transmission estimation, image padding with matting Laplacian matrix (L) [11], is one of the methods that is used in this paper because of similar equa-

tion as fog model represented in (4) also used in He et al. [4]. The refined accurate transmission map $t(z)$ is estimated as:

$$t(z) = k \cdot U \cdot t_0 \quad (11)$$

where L is Laplacian matrix used for matting, k is regularization parameter which is a small value set as 0.0001, so that t is softly constrained by t_0 , where t_0 is the initial estimated transmission map from (9) and U is unit matrix of size same as size of L. Each element o_{ij} of L matrix is defined as [11].

$$L_{ij} = \begin{cases} 0 & i=j \\ -\frac{1}{|w_k|} & i, j \in w_k \end{cases} \quad (12)$$

where P_k is a 3×3 covariance matrix, d_{ij} is the Kronecker delta, I_k is the 3×1 mean vector of the colors I_i and I_j in a window w_k with $|w_k|$ the number of pixels in it, U is 3×3 unit matrix and e is the regularization parameter of small value, set as 10^{-6} assuming the local smoothness which is also account for feature variation in the neighborhood of the reduced feature space.

2.4. Restoration map

The final scene is restored with a little modification in Eq. (5). This modification is required due to the very small value of $t(z)$ (close to zero) which makes the restoration map very prone to noise. Therefore, setting a lower bound value $t_0 = 0.1$ allows for better contrast gain and avoids too small value of $t(z)$. The refined scene reflectance is restored as:

$$I_r = \frac{I_0 - A}{\max\{t, t_0\}} \quad (13)$$

Contrast gain and fine details are still missing in the rough restored map or image using (13) and it needs to improve. Therefore, post-processing performs an important role.

3. Post processing

This section deals with further refinement including local contrast enhancing and increasing the fine detail over the restored image to clearly observe the object in an image. For this purpose, an alternative edge preserving operator, based on WLS filter is used. Camera images are mostly low dynamic range images having smaller range of non linear values. So, here converting Low Dynamic Range (LDR) images into HDR to get amazing detail throughout the tonal range prior to implement WLS filter and compute details of layer, stores the pixel values proportional to the



Fig. 2. Simulation Results with change of x value (a) Original foggy ‘road’ image (b) Output at x = 0.95 of He et al. [4] method (c) Output of proposed method at x = 0.95 shows oversaturated effect (d) Output of proposed method at x = 0.9 shows minimized oversaturation and smooth sky region (e) Output of proposed method at x = 0.5 and (f) at x = 0.2 shows no obvious visibility improvement.

amount of light measured. HDR conversion captures highlights and shadows that may be otherwise lost in a traditional LDR images. To view HDR images on computer, it needs to be converted into a dynamic range using tone mapping. Tone map converts HDR images into RGB format. With this approach, further refinement to eliminate the block artifacts can be achieved and fine details can be revealed.

Edge preserving WLS based smoothing filter may be expressed as the minimum of the following function [12]:

$$L\delta i; j\beta\% \times \delta u_p - r_p\beta^2 \beta k w_{x,p}\delta h\beta - \frac{\sum @u^2}{@x_p} \beta w_{y,p}\delta h\beta - \frac{\sum @u^2}{@y_p} \beta w_{x,p}\delta h\beta \tag{14}$$

where the subscript p represents the spatial location of a pixel. Input image r is rough restored transmission is estimated by a local patch using dark channel method and u is the new refined transmission as an output image. The aim of $\delta u_p - r_p\beta^2$ is to minimize the distance between u and r . The second term tries to achieve smoothness by minimizing the partial derivatives of u . The smoothness requirement is invoked in a spatially varying approach via the smoothness weights $w_{x,p}$ and $w_{y,p}$. A constant value k is used to control smoothing rate as its increasing value results progressively smoother images u . As for smoothness weights, $w_{x,p}\delta h\beta$ and $w_{y,p}\delta h\beta$ are defined as:

$$w_{x,p}\delta h\beta\% \frac{\cdot @L^a}{\cdot @x^p} \beta k^{-1} ; w_{y,p}\delta h\beta\% \frac{\cdot @L^a}{\cdot @y^p} \beta k^{-1} \tag{15}$$

where $L\delta i; j\beta$ is the log-luminance channel of the input image r , exponent a determines the sensitivity of r , while a small constant, k (here set as 10^{-4}) that prevents division by zero in the areas of r . In this article, the value of a is set to 1.2 for the sensitivity.

The minimization of (14) is achieved through the resolution of a linear system of solution as:

$$\delta I \beta k L_r \beta u \% r \tag{16}$$

Therefore, the new output image u is obtained from r as:

$$u \% \delta I \beta k L_r \beta^{-1} r \tag{17}$$

where $L_r \% D_x^T A_x D_x \beta D_y^T A_y D_y$ using matrix notation. Here D_x and D_y are discrete differential operators, and A_x and A_y are diagonal matrices

preserving smoothness. The aim of edge preserving smoothing filter is to get an image u very close to r and as smooth as possible, simultaneously. These two simultaneous actions are contradictory in nature.

3.1. Computation of detail layers and HDR tone mapping

The output fog removed image still has low level of details and looks dark. Hence it is mandatory to compute detail layers and to enhance contrast for which multi-scale edge preserving decomposition [12] has been employed, and that consists of a sequence of difference images resulting into revealing greater details. The detail layers are defined as:

$$d_i \% u_{i-1} - u_i \tag{18}$$

where $i \% 1; 2 \dots m$ and $u_0, u_1, u_2, \dots, u_m$ denote progressively coarser versions of image r with d_0 as base layer and m as detail layers. The roughly restored image r is easily recovered by summing up the base and the detail layers.

$$r \% d_0 \beta \sum_{i=1}^m d_i \tag{19}$$

Here the image (log luminance channel) is decomposed into one base layer and three detail layers multiply each level by some weight to reconstruct a new log luminance image and then converted back into an RGB image. Since the image radiance is not bright and looks darker, therefore, for controlling the exposure we used gamma correction ($c \% 1:5$) with a stronger emphasis on fine details. Gamma correction factor shouldn't be too high or too low to provide the best visual quality on the display unit.

The simulation results at different values of x are presented in Fig. 2. The experiments show that x sometimes needs to be decreased for substantial sky regions in an image, otherwise the sky region may create more artifacts. At $x = 0.9$, the oversaturation in the color quality of an image can also be minimized. The defogging result has no obvious visibility improvement with $x = 0.5$ and $x = 0.2$ as shown in Fig. 2.

4. Simulation results with performance analysis

Simulation and performance evaluation of the proposed algorithm is accomplished through various foggy images processed on MATLAB platform. The proposed algorithm is compared with other previous state of the art methods using qualitative and quantitative evaluation. Quantitative measurement is based on performance parameters. In this article, Contrast Gain (CG) [5,13], Colorfulness Index (CI) [14,15] and Color Information Entropy (CIE) [7] are used as performance metrics for objective evaluation of fog removal algorithm efficiency. Step by step results of the proposed algorithm are shown in Fig. 3, where the final obtained image (Fig. 3(f)) is a fog-free image, while without post-processing the resultant image (Fig. 3(d)) looks dull. The results of intermediate steps show the contribution towards the final restored image. Each intermediate steps has its own importance that helps to improve visibility. Corresponding transmission map and refined transmission map are gray images that depend on object distance from image capturing device. Refinement of transmission map ensures the quality of restored image in Fig. 3(f) after post-processing as compared to the non-refined restored image in Fig. 3(e). The block artifacts in the transmission map (Fig. 3(b)) are refined by capturing discontinuities at sharp edges using the Laplacian matrix and the regularization parameters k and e (see Eqs. (11) and (12)), and are shown in Fig. 3(c). This refinement helps to restore a high quality image with sharp edges

4.1. Contrast gain (CG)

Contrast gain is defined as the mean contrast difference between defogged output and input foggy image. The higher the value of CG, the better is the performance of the algorithm, as it is known that fog-free images have more contrast than the fog affected images. If the mean contrast of the defogged output and the foggy input image of size $M \times N$ are represented by $C_{I,def}$ and $C_{I,fog}$ respectively, then CG is defined as:

$$CG = \frac{C_{I,def} - C_{I,fog}}{C_{I,fog}} \tag{20}$$

and the mean contrast of an image is mathematically expressed as:

$$C_i = \frac{1}{MN} \sum_{j=0}^{M-1} \sum_{k=0}^{N-1} C_{i,j,k} \tag{21}$$

where $C_{i,j,k}$ is the contrast of the pixel at location (i, j) and δ is defined as:

$$C_{i,j,k} = \frac{s_{i,j}}{m_{i,j}} \tag{22}$$

where $m_{i,j}$ and $s_{i,j}$ are behaving like a mean and variance at L_2 norm respectively of an image $I_{i,j}$ as follows:

$$m_{i,j} = \frac{1}{\delta^2} \sum_{k=1}^{\delta} \sum_{l=1}^{\delta} I_{i+k,j+l} \tag{23}$$

and

$$s_{i,j} = \frac{1}{\delta^2} \sum_{k=1}^{\delta} \sum_{l=1}^{\delta} |I_{i+k,j+l} - m_{i,j}|^2 \tag{24}$$

For simulation purpose, δ (5x5 window) is used in this paper to calculate CG.

4.2. Colorfulness Index (CI)

CI is already used for the evaluation of image enhancement techniques [14,15]. In this article, it is used for the first time to evaluate the color quality of fog free images after restoration which includes image enhancement indirectly. The colorfulness index uses a simple opponent color space:

$$r_{g\delta x,y} = R_{\delta x,y} - G_{\delta x,y} \tag{25}$$

and

$$y_{b\delta x,y} = \frac{1}{\delta} (R_{\delta x,y} + G_{\delta x,y} + B_{\delta x,y}) \tag{26}$$

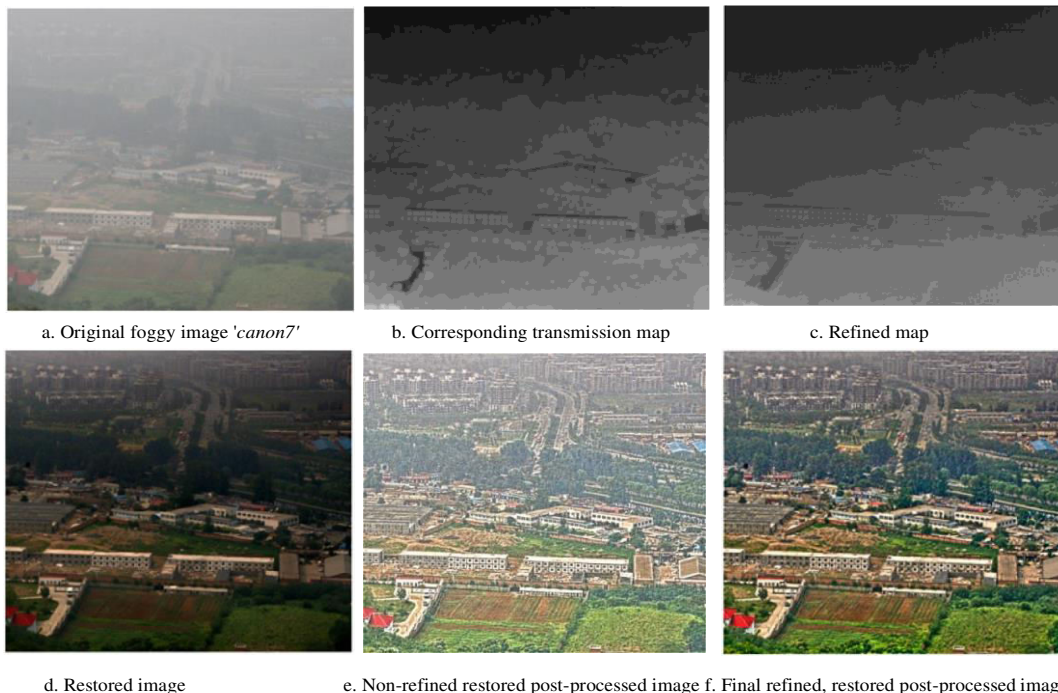


Fig. 3. Step by step results of proposed algorithm.

The Colorfulness Index (CI) for an image (here defogged) is given by:

$$CI = \frac{1}{3} \sqrt{\frac{r_{rgb}^2 + g_{rgb}^2 + b_{rgb}^2}{\mu_{rgb}^2}}$$

where; $r_{rgb} = \sqrt{\frac{1}{3} \sum_{i=1}^n (r_i - \mu_r)^2}$ δ28p

and

$$\mu_{rgb} = \frac{1}{n} \sum_{i=1}^n r_i$$
δ29p

where r is the standard deviation and μ is the mean of the pixels included in the image. An increased value of CI induces a greater visibility which is larger in fog free images as compared to foggy images. It also indicates better performance of fog removal algorithm in terms of degree of color quality.

4.3. Color Information Entropy (CIE)

Entropy is a statistical measure of randomness that can be used to characterize the texture of the input image. It can be determined from the histogram of an image of all gray levels; however the image may be two dimensional or multidimensional. The CIE represents the amount of information in a color image. CIE attains its maximum value when an image is non uniform but for a foggy or haze containing areas in an image has minimal CIE. CIE is mathematically defined as:

$$CIE = -\sum_{k=0}^{L-1} P_k \log_2 P_k$$
δ30p

where L is the number of gray levels and P_k is the probability associated with gray level k or histogram count. A foggy or a hazy image contains little amount of texture information as compared to fog free images and hence the CIE value will be greater for the restored image comparatively. Thus, CIE shows the effectiveness of any fog removal algorithm. Qualitative performance comparison of the proposed algorithm with other existing techniques is shown in

Figs. 4 and 5 with intense fog ('canon7') and mild fog ('ny17') images respectively.

The proposed algorithm shows clear details of fog free scene objects as compared to other methods with acceptable visual quality without sky region or less sky region images with intense fog like 'canon7'. The resultant image of the proposed method in Fig. 5 contains few amount of unnatural color near the sky region that is also present in Fattal's [8] but the dark tree region (shown in small pillbox) becomes clearer in the proposed method. Un-natural color near sky region can be negligible when it is applied for FVES and another similar kind of applications where fog removal has a greater impact than the presence of a little amount of unnatural color as it occurs due to the sky region.

Simulation is carried out on a number of different kind of scenes containing fog and the comparative quantitative analysis of CG, CI and CIE on seven different images, 'ny17', 'y01', 'y16', 'canon7', 'cityscape', 'K-080-000005' (synthetic image [17]) and 'road' are shown in Tables 1, 2 and Fig. 6. The last two figures in Tables 1 and 2 represents the road images considered as street scene.

The proposed algorithm is compared with other previous well-known techniques except Negru et al., qualitatively (see Figs. 4 & 5) and quantitatively as shown in Tables 1 and 2. A more recent one [17] compared their proposed method with the different set of parameters and fog density variation mostly on synthetic images and hence it is not compared with the proposed technique. The proposed algorithm produces higher values of CG and CI as compared to other state of the art methods for all types of images. Higher values of CG shows better contrast which indicates a gap of contrast between foggy and fog free image. Higher values of CI greatly preserve the color quality of a fog-free image. The algorithms are arranged from left to right (Table 1) according to an average increase in their performance as well as from early to latest year of research. Colored bar graphs (Fig. 6) also show that the proposed fog removal method produces higher CG and higher CI. It ensures the efficiency of the proposed single image fog removal algorithm. CIE is also evaluated as shown in Table 2 for

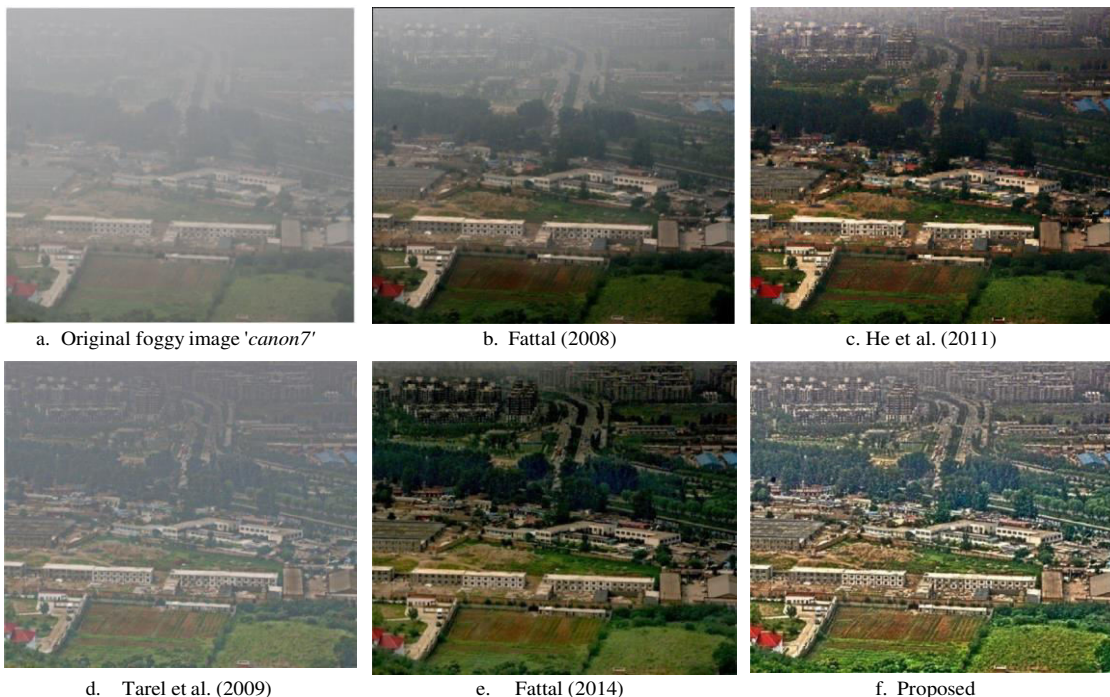


Fig. 4. Qualitative performance comparison of proposed algorithm with other existing algorithms.

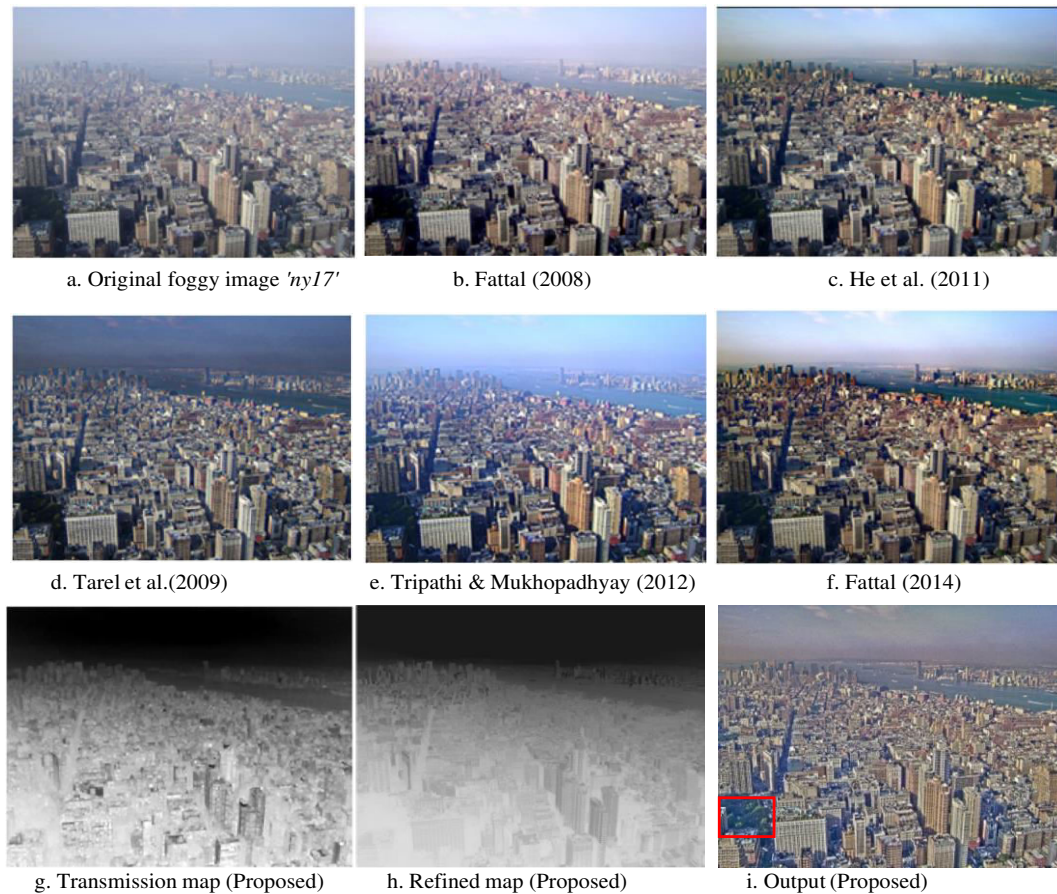


Fig. 5. Qualitative performance comparison of proposed algorithm with state-of-art algorithms.

Table 1
Comparison of CG and CI produced by proposed and previous competing algorithms on different images.

Images	Methods											
	Fattal [2]		He et al. [4]		Tarel et al. [3]		Tripathi and Mukhopadhyay [5]		Fattal [8]		Proposed	
	CG	CI	CG	CI	CG	CI	CG	CI	CG	CI	CG	CI
'ny17'	0.102	14.160	0.093	15.835	0.116	13.398	0.165	14.889	0.0808	22.201	0.170	23.153
'y01'	0.061	13.476	0.086	14.514	0.084	13.532	0.111	13.182	0.0389	21.444	0.124	22.913
'y16'	0.039	9.833	0.068	17.497	0.091	13.626	0.146	13.347	0.0215	17.490	0.093	18.778
'canon7'	0.010	16.982	0.019	12.873	0.021	13.870	-	-	0.0217	31.013	0.146	34.019
'cityscape'	-	-	0.035	27.06	0.027	23.335	-	-	0.0680	22.83	0.087	34.30
'K-080-000005'	-	-	0.016	12.88	0.033	15.17	-	-	-	-	0.018	20.22
'road'	-	-	0.019	14.023	0.033	11.87	-	-	0.083	19.18	0.087	19.4

Table 2
Comparison of CIE evaluated by proposed and previous competing algorithms on different images.

Images	Methods						
	Input	Fattal [2]	He et al. [4]	Tarel et al. [3]	Tripathi and Mukhopadhyay [5]	Fattal [8]	Proposed
	Color Information Entropy (CIE)						
'ny17'	7.6129	7.6858	7.8853	7.5523	7.6849	7.6418	7.6319
'y01'	7.5563	7.7521	7.4384	7.6889	7.6798	7.5883	7.4963
'y16'	7.6291	7.7048	7.7625	7.8195	7.6397	7.5922	7.5379
'canon7'	6.4315	7.4451	5.1333	6.3013	-	6.3355	7.4926
'cityscape'	6.3646	-	7.2068	5.0273	-	7.4286	7.5609
'K-080-000005'	4.4887	-	4.3880	4.3648	-	-	6.3872
'road'	7.3410	-	7.5716	5.8018	-	7.5015	7.6225

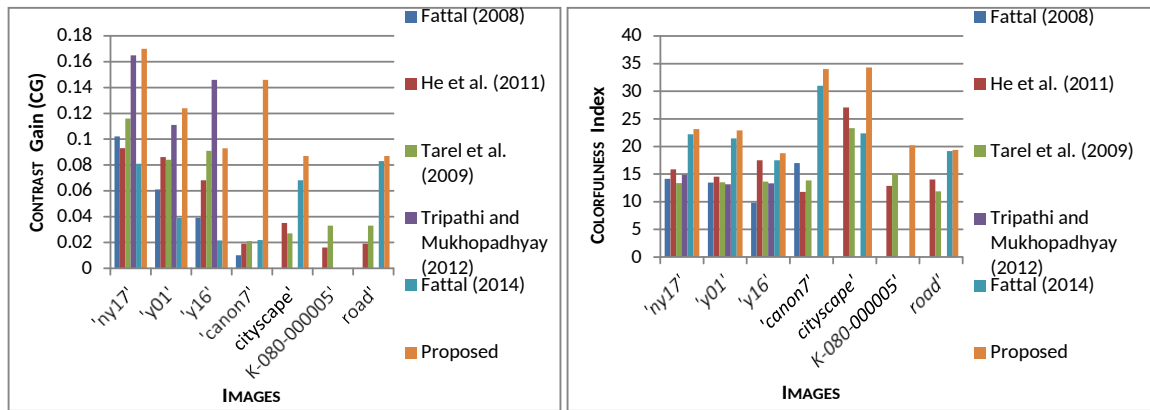


Fig. 6. Comparative CG (left) and CI (right) of seven different foggy images using existing and proposed fog removal algorithms.

Table 3
Quantitative evaluation at different values of 'x'.

Quantitative Indexes	Input foggy image	Output at 'x'				
		'road'	He et al. [4], (x = 0.95)	Proposed (x = 0.95)	Proposed (x = 0.9)	Proposed (x = 0.5)
Color Information Entropy (CIE)	7.34	7.57	7.58	7.62	6.85	6.20
Colorfulness Index (CI)	6.98	14.02	21.43	19.4	6.95	4.43
Contrast Gain (CG)	-	0.019	0.084	0.087	0.052	0.014

comparative analysis of single image defogging algorithms along with the proposed method. CIE is a positive quantity and its values for 'canon7', 'cityscape', 'K-080-000005' and 'road' are greater in the proposed method than all other existing algorithms. For image 'ny17', CIE of the proposed method is greater than Tarel et al. [3], and approximately same as Fattal's [8].

The reduction of CIE in the proposed method for the rest of two images ('y01' and 'y16') is possible only because of they contain a larger area of sky region as compared to 'ny17' and 'canon7'. Most of the existing methods have the same problem with the sky region as the atmospheric light is very close to sky color and erroneously it is considered as a layer of fog.

All the simulations of the proposed method have been carried out at fixed x with x = 0.9. The variation of x also affects the quantitative indexes viz. CIE, CI and CG as shown in Table 3 in addition to the visual effects (see Fig. 2). CIE and CG of the proposed method for 'road' image at x = 0.9 are better than other values of x. CI of the proposed method at x = 0.9 doesn't show oversaturation in the color quality of the image. It may be noted that the value of x is application based and for the Fog Vision Enhancement System reported here, best performance has been achieved with x = 0.9.

In this article, post processing is not just like a simple histogram stretching [5] that only increases the contrast in an image without preserving more details but the prior converted HDR image with WLS filter is used to enhance the details in the captured image. Pre-processing is even not required for contrast stretching in the proposed technique as it is introduced in Tripathi and Mukhopadhyay [5]. Proposed scheme maintains the color quality without any pre-processing step, however a little oversaturation in few images is observed due to the conversion into HDR. This amount of oversaturation in few images can be neglected in comparison to the amount of fog removal. Another drawback of the proposed algorithm is that it is best suitable only for those images containing small sky regions. The proposed method also uses a Laplacian operator with fixed kernel coefficients for edge detection and estimation without any kind of user intervention.

5. Conclusions

Single image fog removal is one of the basic and important tasks to develop a robust and versatile computer vision system for object tracking, traffic sign recognition system and FVES. In this research article, a novel and efficient single image fog removal algorithm is proposed for both gray and color images. The proposed method uses HDR conversion of image before preserving the details using WLS filter and shows pleasant output image. Different kinds of scenes under fog condition are tested and the values of gamma correction factor with other coefficients are chosen appropriately to make the proposed method more efficient. The efficiency of the proposed method is verified using subjective and objective evaluation with fixed and variable x. Simulation results and analysis shows that the output fog-free image contains more clear edges with details and better contrast. It also preserves color quality for RGB images and other image transformation models (YUV, HSV, CMYK etc.) seem to produce similar results. Fog removal algorithms are easy to implement for a single image rather than on a video however, it can be extended using motion estimation.

Acknowledgements

The fatal crashes statistics is provided by National Highway Traffic Safety Administration (NHTSA). The authors would like to thank Lyn Cianflocco, National Highway Traffic Safety Administration, National Center for Statistics & Analysis Data Reporting & Information Division, USA for providing the fatal motor vehicle traffic crashes data during five years from 2009-2013 based on different weather conditions. The authors also would like to thank the reviewers and the editor for their valuable comments.

References

[1] Y.Y. Schechner, et al., Instant dehazing of images using polarization, Computer Vision and Pattern Recognition, in: Proc. IEEE Computer Society Conference, 1 (2001), pp. 1-325.
 [2] R. Fattal, Single image dehazing, ACM Trans. Graph. 27 (3) (2008) 72.

- [3] J.P. Tarel, N. Hautiere, Fast visibility restoration from a single color or gray level image, in: Proc. 12th IEEE International Conference on Computer Vision, pp. 2201–2208 (2009).
- [4] K. He et al., Single image haze removal using dark channel prior, *IEEE Trans. Pattern Anal. Mach. Intell.* 33 (12) (2011) 2341.
- [5] A.K. Tripathi, S. Mukhopadhyay, Single image fog removal using anisotropic diffusion, *IET Image Proc.* 6 (7) (2012) 966–975.
- [6] C. Ancuti, Ancuti, Single image dehazing by multi-scale fusion, *IEEE Trans. Image Process.* 22 (8) (2013) 3271–3282.
- [7] Y. Wang, C. Fan, Single image defogging by multiscale depth fusion, *IEEE Trans. Image Process.* 23 (11) (2014) 4826–4837.
- [8] R. Fattal, Dehazing using color-lines, *ACM Trans. Graph.* 34 (1) (2014) 13.
- [9] R. Lagendijk et al., Regularized iterative image restoration with ringing reduction, *IEEE Trans. Acoust. Speech Signal Process.* 36 (12) (1988) 1874–1888.
- [10] W.K. Middleton, *Vision through the Atmosphere* (1957).
- [11] A. Levin et al., A closed-form solution to natural image matting, *IEEE Trans. Pattern Anal. Mach. Intell.* 30 (2) (2008) 228–242.
- [12] Z. Farbman et al., Edge-preserving decompositions for multi-scale tone and detail manipulation, *ACM Trans. Graph.* 27 (3) (2008) 67.
- [13] T.L. Economopoulos et al., Contrast enhancement of images using partitioned iterated function systems, *Image Vis. Comput.* 28 (1) (2010) 45–54.
- [14] D. Hasler, S.E. Suesstrunk, Measuring colorfulness in natural images, *Electronic Imaging International Society for Optics and Photonics*, 2003. pp. 87–95.
- [15] J. Xu et al., Image enhancement using two gamma-rescaling curves and multi-scale Gaussian matrix, in: *International Conference on Intelligent and Advanced Systems*, (2007) pp. 709–713.
- [16] Lee et al., A Review on dark channel prior based image dehazing algorithms, *EURASIP J. Image Video Process.* 1 (2016) 1–23.
- [17] M. Negru et al., Exponential contrast restoration in fog conditions for driving assistance, *IEEE Trans. on ITS* 16 (4) (2015).